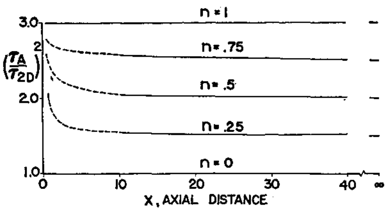

Fig. 1 Ratio of laminal shear stess for two-dimensional and axially symmetric bodies of the form $r = x^n$

and

$$s = \int_0^s \left[1 + \left(\frac{dr}{dx}\right)^2\right]^{1/2} dx$$

one can transpose Eq. (1) to the axis of symmetry as follows:

$$\frac{\tau_A}{\tau_{2D}} = \left[\frac{r^2(x) \int_0^x [1 + (dr/dx)^2]^{1/2}\, dx}{\int_0^x r^2(x)\, [1 + (dr/dx)^2]^{1/2}\, dx}\right]^{1/2} \qquad (2)$$

For the class of bodies considered in this note, namely, $r = x^n$, Eq. (2) may be expressed as

$$\left(\frac{\tau_A}{\tau_{2D}}\right)^2 = \frac{X^{2n} \int_0^x [1 + n^2x^{2(n-1)}]^{1/2}\, dx}{\int_0^x x^{2n}[1 + n^2x^{2(n-1)}]^{1/2}\, dx} \qquad (3)$$

Although direct integration of Eq. (3) is not possible (except for $n = 0, \frac{1}{2}, 1$, and 2), some results of a 16-point Gaussian numerical integration are shown in Fig. 1. [It is noted that the basic assumption that the body dimension must be much greater than the boundary layer thickness limits the accuracy of Eq. (3) at small values of x.] It is possible to examine the limits of this expression by applying l'Hospital's rule. Inspection of Eq. (3) reveals that a series expansion is divergent for values of n greater than 1.0; hence, l'Hospital's rule is valid in this work for the condition $n \leq 1$:

$$\lim_{x\to a} \left(\frac{\tau_A}{\tau_{2D}}\right)^2 =$$

$$\lim_{x\to a} \left[\frac{[1 + n^2x^{2(n-1)}]^{1/2} + (2n/x)\int_0^x [1 + n^2x^{2(n-1)}]^{1/2}\, dx}{[1 + n^2x^{2(n-1)}]^{1/2}}\right] \qquad (n \leq 1) \quad (4)$$

Rearranging Eq. (4) and applying the rule again, one obtains the following:

$$\lim_{x\to a}\left(\frac{\tau_A}{\tau_{2D}}\right)^2 - 1 = \lim_{x\to a}\left\{\frac{2n[1 + n^2x^{2(n-1)}]}{[1 + n^3x^{2(n-1)}]}\right\} \quad (n \leq 1) \qquad (5)$$

This equation reduces to

$$\underset{x\to\infty}{(\tau_A/\tau_{2D})} = [1 + 2n]^{1/2} \qquad (n \leq 1) \quad (6)$$

It is important to note that Eq. (3) is an important parameter in laminar aerodynamic heating and laminar shear stress calculations but is much too cumbersome to be a useful engineering tool. Equation (6), however, is a sufficiently simple expression to be a useful tool. Also, Eq. (6) yields reasonably accurate results well into the area of doubtful validity of Eq. (3) (at small values of x).

Evaluation of both Eqs. (3) and (6) for $n = 0$ (cylinder) and $n = 1$ (cone) yields

$$\tau_A/\tau_{2D} = \underset{x\to\infty}{\tau_A/\tau_{2D}} = 1$$

and

$$\tau_A/\tau_{2D} = \tau_A/\tau_{2D} = 3^{1/2}$$

respectively. These results agree with Mangler's work.

τ_A may be determined after establishing an adequate pressure gradient (Newtonian, tangent cone, test data, etc.) and solving for τ_{2D}. This work, which is beyond the intended scope of this note, is in progress.

Circular Orbit Partial Derivatives

Wayne H. Tempelman*
Lockheed Missiles and Space Company, Palo Alto, Calif.

Circular orbit partial derivatives are presented in both rotating and nonrotating coordinate systems for the following cutoff conditions: time, angle, and downrange distance. The accuracy of propagating errors through the partials depends on the coordinate system chosen, with the most accurate propagation being in the polar coordinate system.

I. Introduction

BALLISTIC orbit accuracy analysis involves propagation of initial errors either in the form of a state vector or in the form of a covariance matrix through a matrix of partial derivatives to determine the final error. The partial derivatives depend on the cutoff condition that is determined by the mission. Examples of cutoff conditions are time (deboost from orbit at a specified time) and downrange distance (deboost from orbit using a satellite mapping device). Preceding the presentation of the partials are discussions of different coordinate systems and the differences between rotating and nonrotating coordinate systems.

II. Coordinate Systems

A family of curvilinear orthogonal coordinate systems is illustrated in Fig. 1, where one of the axes is a straight line normal to the velocity vector, and the other axis passes through the nominal point perpendicular to the first and consists of an arc of a circle which curves inward toward the attracting body. These coordinate systems have the common feature that, about the nominal point, they are all equivalent to first order. Any first-order perturbation analysis about the nominal point therefore is independent of which one of this family is chosen and will result in the same matrix of partials. An initial error propagated in the different members of the family will result in a locus of possible final errors, all correct to the first order. An example is illustrated in Fig. 1. Since the correct final error lies close to the nominal orbit, and since the curvilinear coordinate system with radius equal to the radius of the circular orbit follows the nominal trajectory exactly, this coordinate system will result in a more accurate prediction of the final error than any of the other curvilinear coordinate systems. This coordinate system is the polar coordinate system used in Refs. 1–3.

To show analytically that this solution is identical to the Cartesian coordinate system (a limiting member of the forementioned family) used in Refs. 4–6, consider the following

---

Received by ARS August 9, 1962; revision received February 15, 1963. The author wishes to express his appreciation to H. P. Mickelsen for having suggested the possibility of improved accuracy using the polar coordinate system and to R. C. Rosenbaum for several clarifying discussions.

* Senior Dynamics Engineer, Flight Mechanics Group, Mechanical and Mathematical Sciences Laboratory.

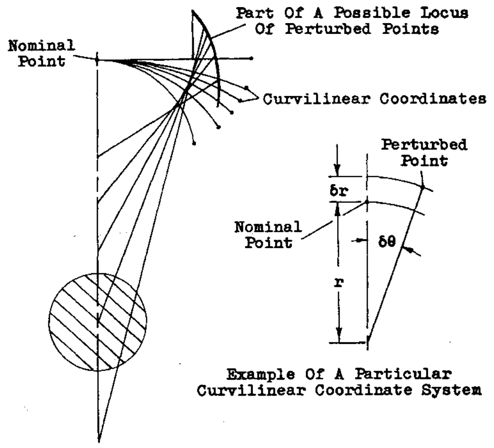

Fig. 1 Possible curvilinear coordinate systems

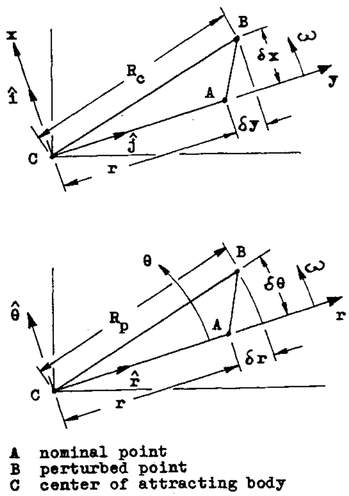

Fig. 2 Rotating Cartesian and polar coordinate notation

initial position vectors in the two rotating coordinate systems obtained from Fig. 2:

$$
\begin{aligned}
R_p &= r\delta\theta\hat{\theta} + (r + \delta r)\,\hat{r} \\
R_c &= \delta x\hat{\imath} + (r + \delta y)\hat{\jmath}
\end{aligned}
\tag{1}
$$

Capital letters will be used for all vectors except for the unit vectors $\hat{\imath}, \hat{\jmath}, \hat{r}$, and $\hat{\theta}$. Differentiating, dropping the second-order terms, and considering that the unit vectors rotate with ωt,

$$
\begin{aligned}
\dot{R}_p &= (r\delta\dot{\theta} + \omega\delta r + \omega r)\hat{\theta} + (\delta\dot{r} - \omega r\delta\theta)\hat{r} \\
\dot{R}_c &= (\delta\dot{x} + \omega\delta y + \omega r)\hat{\imath} + (\delta\dot{y} - \omega\delta x)\hat{\jmath} \\
\ddot{R}_p &= (r\delta\ddot{\theta} + 2\omega\delta\dot{r} - \omega^2 r\delta\theta)\hat{\theta} + \\
&\qquad (\delta\ddot{r} - 2\omega r\delta\dot{\theta} - \omega^2\delta r - \omega^2 r)\hat{\jmath} \\
\ddot{R}_c &= (\delta\ddot{x} + 2\omega\delta\dot{y} - \omega^2\delta x)\hat{\imath} + \\
&\qquad (\delta\ddot{y} - 2\omega\delta\dot{x} - \omega^2\delta y - \omega^2 r)\hat{\jmath}
\end{aligned}
\tag{2}
$$

The solution is obtained from Newton's law of gravity:

$$
F = m\ddot{R} = -Gm\,Mr^{-3}R \tag{3}
$$

Expanding r^{-3} and dropping the second-order terms,

$$
\begin{aligned}
r_p^{-3} &= (r + \delta r)^{-3} \cong r^{-3}(1 - 3r^{-1}\,\delta r) \\
r_c^{-3} &= [x^2 + (r + \delta y)^2]^{-3/2} \cong r^{-3}(1 - 3r^{-1}\delta y)
\end{aligned}
\tag{4}
$$

By examining Eqs. (1, 2, and 4), it is seen that one set of equations can be obtained from the other with the substitution

$$
\begin{bmatrix} \delta x \\ \delta y \\ \delta\dot{x} \\ \delta\dot{y} \end{bmatrix} = \begin{bmatrix} r\delta\theta \\ \delta r \\ r\delta\dot{\theta} \\ \delta\dot{r} \end{bmatrix} \equiv \begin{bmatrix} \delta R \\ \delta V \end{bmatrix} \equiv [X] \tag{5}
$$

Hence, upon solving the differential equations of Eq. (3), an identical matrix of partial derivatives will be obtained in each coordinate system.

It should be noted that the polar coordinate solution can be transformed into a Cartesian coordinate solution with a nonlinear set of equations resulting. A comparison (Fig. 3), used in Ref. 6 to illustrate the inaccuracies of the Cartesian coordinate solution, shows a marked improvement in accuracy using the polar coordinate solution.

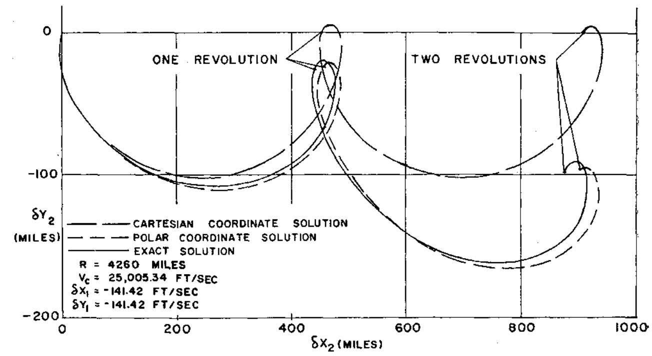

Fig. 3 Comparison of exact solution with two approximate solutions

III. Rotating and Nonrotating Coordinate Systems

The analysis of the partial derivatives can be made in either a rotating or a nonrotating, otherwise similar, coordinate system. Different matrices of partials will result, and the state vector error (X) will be different in each case. The nonrotating X is that X which would be observed from the nonrotating coordinate system and consists of the state vector on the perturbed orbit minus the state vector on the circular orbit. The rotating X is the state vector of the perturbed orbit as observed from the nominal point on the rotating coordinate system. The errors are related by the matrix equation

$$
\delta V_n = \delta V_r - \Omega\delta R \qquad \delta R = \delta R_n = \delta R_r \tag{6}
$$

where

$$
\Omega = \begin{bmatrix} 0 & -\omega \\ \omega & 0 \end{bmatrix}
$$

and n refers to the nonrotating coordinate system and r to the rotating coordinate system. Equation (6) shows how the vector δR and its derivative with respect to time (δV) appear in coordinate systems that differ only in their rotational rate.[7]

The partials in the rotating coordinate system can be obtained from the partials in the nonrotating coordinate system or vice versa, by substituting in the expression

$$
\begin{bmatrix} \delta R \\ \delta V \end{bmatrix}_2 = \begin{bmatrix} P_1 & P_2 \\ P_3 & P_4 \end{bmatrix} \begin{bmatrix} \delta R \\ \delta V \end{bmatrix}_1 \tag{7}
$$

the proper terms from Eq. (6). For example,

$$
\begin{bmatrix} \delta R \\ \delta V \end{bmatrix}_{2_r} = \begin{bmatrix} P_1 - P_2\Omega & P_2 \\ P_3 - P_4\Omega + \Omega P_1 - \Omega P_2\Omega & P_4 + \Omega P_2 \end{bmatrix} \begin{bmatrix} \delta R \\ \delta V \end{bmatrix}_{1_r} \tag{8}
$$

when the partials are expressed in the nonrotating coordinate system.

For either of the coordinate systems illustrated in Fig. 4, the following matrices give the circular orbit time cutoff partials for rotating and nonrotating coordinate systems, respectively:

$$[X_2] = \begin{bmatrix} 1 & 6(\sin\omega t - \omega t) & \omega^{-1}(4\sin\omega t - 3\omega t) & 2\omega^{-1}(\cos\omega t - 1) \\ 0 & 4 - 3\cos\omega t & 2\omega^{-1}(1 - \cos\omega t) & \omega^{-1}\sin\omega t \\ 0 & 6\omega(\cos\omega t - 1) & 4\cos\omega t - 3 & -2\sin\omega t \\ 0 & 3\omega\sin\omega t & 2\sin\omega t & \cos\omega t \end{bmatrix} [X_1] \quad (9)$$

$$[X_2] = \begin{bmatrix} 2\cos\omega t - 1 & 2\sin\omega t - 3\omega t & \omega^{-1}(4\sin\omega t - 3\omega t) & 2\omega^{-1}(\cos\omega t - 1) \\ \sin\omega t & 2 - \cos\omega t & 2\omega^{-1}(1 - \cos\omega t) & \omega^{-1}\sin\omega t \\ -\omega\sin\omega t & \omega(\cos\omega t - 1) & 2\cos\omega t - 1 & -\sin\omega t \\ \omega(1 - \cos\omega t) & \omega(3\omega t - \sin\omega t) & 3\omega t - 2\sin\omega t & 2 - \cos\omega t \end{bmatrix} [X_1] \quad (10)$$

In addition to being able to derive the nonrotating partials from the rotating partials by the method of Eq. (8), they can be derived from the two-body equations of motion expressed in an arbitrary nonrotating Cartesian coordinate system.[8] After differentiation, they can be transformed into the coordinate system illustrated in Fig. 4 by having the initial point occur on the y axis and then by multiplying the matrix of partials by the transformation matrix involving $\theta = \omega t$.

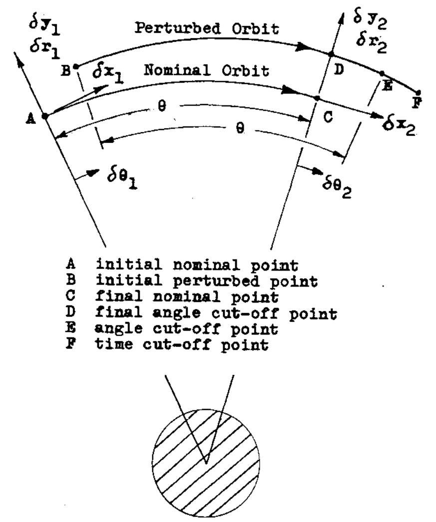

Fig. 4 Coordinate systems and cutoff conditions for circular orbits

IV. Angle Cutoff Condition

The foregoing matrices were derived on the basis of time being the cutoff condition; i.e., the final position on the perturbed orbit was determined by having the time on the perturbed orbit equal to the time on the nominal orbit. Angle-dependent partials can be derived on the basis of the final position on the perturbed orbit being determined by having the same range angle as on the nominal orbit (see Fig. 4). In the coordinate systems illustrated in Fig. 4, the following matrices give the circular orbit partials for the angle cutoff condition in the rotating and nonrotating coordinate systems, respectively:

$$[X_2] = \begin{bmatrix} 1 & 0 & 0 & 0 \\ 0 & 4 - 3\cos\theta & 2\omega^{-1}(1 - \cos\theta) & \omega^{-1}\sin\theta \\ 0 & 6\omega(\cos\theta - 1) & 4\cos\theta - 3 & -2\sin\theta \\ 0 & 3\omega\sin\theta & 2\sin\theta & \cos\theta \end{bmatrix} [X_1] \quad (11)$$

$$[X_2] = \begin{bmatrix} 1 & 0 & 0 & 0 \\ \sin\theta & 2 - \cos\theta & 2\omega^{-1}(1 - \cos\theta) & \omega^{-1}\sin\theta \\ -\omega\sin\theta & \omega(\cos\theta - 1) & 2\cos\theta - 1 & -\sin\theta \\ \omega(\cos\theta - 1) & \omega\sin\theta & 2\sin\theta & \cos\theta \end{bmatrix} [X_1] \quad (12)$$

A final angle cutoff condition (i.e., cutoff on downrange distance) results in a cutoff point that occurs directly above the final nominal point, as shown in Fig. 4. Reference 9 contains the nonrotating coordinate system partials for the final angle cutoff condition. The rotating partials are identical to the angle partials given in Eq. (11) except for $\partial x_2/\partial x_1 = 0$, and the nonrotating partials to those in Eq. (12) except for $\partial x_2/\partial x_1 = 0$ and $\partial \dot{y}_2/\partial x_1 = \omega\cos\theta$.

V. Out-Of-Plane Analysis

The out-of-plane analysis is independent of the foregoing considerations and results in the matrix of partials

$$\begin{bmatrix} \delta z_2 \\ \delta \dot{z}_2 \end{bmatrix} = \begin{bmatrix} \cos\theta & \omega^{-1}\sin\theta \\ -\omega\sin\theta & \cos\theta \end{bmatrix} \begin{bmatrix} \delta z_1 \\ \delta \dot{z}_1 \end{bmatrix} \quad (13)$$

References

[1] Braham, H. and Skidmore, L., "Guidance-error analysis of satellite trajectories," J. Aerospace Sci. **29**, 1091–1101 (1962).

[2] Wisneski, M. L., "Error matrix for a flight on a circular orbit," ARS J. **32**, 1416–1418 (1962).

[3] Duke, W., Goldberg, E., and Pfeffer, I., "Error analysis considerations for a satellite rendezvous," ARS J. **31**, 505–513 (1961).

[4] Wheelon, A. D., "Midcourse and terminal guidance," *Space Technology* (John Wiley and Sons, Inc., New York, 1959), Chap. 26, p. 31.

[5] Lieberman, S. I., "Rendezvous acceptability regions based on energy considerations," ARS J. **32**, 287–290 (1962).

[6] Eggleston, J. M. and Beck, H. D., "A study of the positions and velocities of a space station and a ferry vehicle during rendezvous and return," NASA TR-R-87 (1961).

[7] Goldstein, H., *Classical Mechanics* (Addison-Wesley Publishing Co., Cambridge, Mass., 1953), pp. 132–133.

[8] Herrick, C. E. and R. Leger, "Trajectory computation in systems design," *Space Trajectories* (Academic Press, New York, 1960), pp. 127–140.

[9] Tempelman, W. H., "Selected problems in optimum ballistic descent from orbit," Astronaut. Acta **VIII**, 193–204 (1962).